Carbohydrate Polymers 93 (2013) 499–505

Contents lists available at SciVerse ScienceDirect

Carbohydrate Polymers

journal homepage: www.elsevier.com/locate/carbpol

Polysaccharide nanofiber made from euglenoid alga

Motonari Shibakami[a,*], Gen Tsubouchi[a], Makoto Nakamura[b], Masahiro Hayashi[c]

[a] Biomedical Research Institute, National Institute of Advanced Industrial Science and Technology (AIST), Central 6th, 1-1-1 Higashi, Tsukuba, Ibaraki 305-8566, Japan
[b] Industrial Technology Center of Wakayama Prefecture, Ogura 60, Wakayama, Wakayama 649-6261, Japan
[c] Department of Marine Biology and Environmental Science, Faculty of Agriculture, University of Miyazaki, 1-1 Gakuen Kibanadai-nishi, Miyazaki, Miyazaki 889-2192, Japan

ARTICLE INFO

Article history:
Received 26 October 2012
Received in revised form 7 December 2012
Accepted 12 December 2012
Available online 26 December 2012

Keywords:
Nanofiber
Polysaccharide
β-1,3-Glucan
Paramylon
Euglena

ABSTRACT

We have fabricated a polysaccharide nanofiber made from paramylon (β-1,3-glucan), a storage polysaccharide stored as a micrometer-sized particle in the cell of euglenoid alga. Preparation of this nanofiber primarily hinges on the bottom-up approach. First, paramylon, which is originally present in the form of a bundle of nanofibers in a particle, was fibrillated to a randomly coiled polymer by dissolving the particle in a 1.0-mol/L NaOH aqueous solution. Second, the randomly coiled polymer was allowed to self-assemble into a triplex as the NaOH concentration was reduced to 0.25–0.20 mol/L. Third, a 20-nm-width nanofiber made from the triplex emerged in the solution when the NaOH concentration was reduced to approximately 0.20 mol/L.

1. Introduction

One major goal of modern material chemistry is to find ways to fabricate nanofibers (Hong, Um, Nam, Hong, & Lee, 2009; Kim, Rothschild, Lee, Kim, Jo, & Tuller, 2006; Li & Kaner, 2005; Loscertales, Barrero, Marquez, Spretz, Velarde-Ortiz, & Larsen, 2004; Wnek, Carr, Simpson, & Bowlin, 2003; Zhang, Goux, & Manohar, 2004). Polysaccharide nanofibers have drawn particular attention because of their mechanical strength, biodegradability, and environmental friendliness (Bhatnagar & Sain, 2005; Chen, Wang, Wei, Mo, & Cui, 2010; Cooper, Zhong, Kinoshita, Morrison, Rolandi, & Zhang, 2012; Iwatake, Nogi, & Yano, 2008; Ohkawa, Minato, Kumagai, Hayashi, & Yamamoto, 2006; Zhang, Wang et al., 2010). Cellulose nanofibers are one of the most intensively studied polysaccharide nanofibers. Preparation of these nanofibers requires fibrillation of plant fibers using a top-down approach such as a mechanical treatment or enzymatic method (Bhatnagar & Sain, 2005; Chakraborty, Sain, & Kortschot, 2005; Paakko et al., 2007; Taniguchi & Okamura, 1998; Zhao, Feng, & Gao, 2007). This approach, however, results in aggregated nanofibers with a width distribution that is too wide because of the complicated multilayered structure of plant fibers and the interfibrillar hydrogen bonds.

Various fibrillation methods have been devised to overcome this problem (Abe, Iwamoto, & Yano, 2007; Saito & Isogai, 2004). Our efforts in this area have focused on using a bottom-up approach in which components automatically self-assemble into well-organized structures. We used β-1,3-glucans as a component of polysaccharide nanofibers because many of these glucans have an inherent self-assembling ability that enables the glucans to form a triplex and micro- or nanofibers (Barras & Stone, 1968; Brandes, Buetow, Bertini, & Malkoff, 1964; Chuah, Sarko, Deslandes, & Marchessault, 1983; Clarke & Stone, 1960; Falch & Stokke, 2001; Kashiwagi, Norisuye, & Fujita, 1981; Numata et al., 2006; Ogawa, Ono, Watanabe, & Tsurugi, 1972; Ogawa, Tsurugi, & Watanabe, 1972; Saito, Ohki, & Sasaki, 1979; Saito, Ohki, Takasuka, & Sasaki, 1977; Stokke, Falch, & Dentini, 2001; Wang, Zhang, Zhang, & Ding, 2009; Yanaki, Kojima, & Norisuye, 1981; Zhang, Li, Zhou, Zhang, & Chen, 2002; Zhang, Zhang, Zhou, Zhang, Zhang, & Li, 2001; Zhang, Li, & Zhang, 2010). Our working hypothesis has been that β-1,3-glucans may be of practical use as durable resources if they do not have branched sugar chains that may increase water-solubility and if the micro- or nanofibers they form have sufficient mechanical strength. With this hypothesis in mind, we have started a program aimed at testing the feasibility of paramylon, a β-1,3-glucan produced by a euglenoid alga, as a component of a practical nanofiber. Our reasons for choosing this polysaccharide were twofold. First, while nearly all other β-1,3-glucans have, more or less, branched chains, paramylon is strictly a linear polysaccharide (Booy, Chanzy, & Boudet, 1981; Clarke & Stone, 1960; Harada, Misaki, & Saito, 1968; Kobayashi, Kimura, Togawa, Wada, & Kuga, 2010; Kreger & Meeuse, 1952; McIntosh, Stone, & Stanisich, 2005; Saito, Misaki, & Harada, 1968). Thus, paramylon meets the linearity requirement. Second, bulk production may be possible since this polysaccharide is produced in significant quantities by readily cultured euglenoid alga

* Corresponding author. Tel.: +81 29 861 4547; fax: +81 29 861 4547.
E-mail address: moto.shibakami@aist.go.jp (M. Shibakami).

0144-8617/$ – see front matter © 2012 Elsevier Ltd. All rights reserved.
http://dx.doi.org/10.1016/j.carbpol.2012.12.040

(Barsanti, Vismara, Passarelli, & Gualtieri, 2001; Santek, Friehs, Lotz, & Flaschel, 2012).

Our ultimate goal has been to prepare paramylon nanofiber-based durables. To this end, the immediate aim of the work reported here was to demonstrate that paramylon can form a nanofiber in vitro. In this article, we describe the conformational analysis of paramylon, examine the feasibility of the dilution method as a means of forming a paramylon nanofiber, and discuss the structure of the nanofiber in detail. We also briefly discuss the self-assembly process of paramylon from randomly coiled β-1,3-glucans to a nanofiber and the nanofiber structure.

2. Experimental

2.1. General methods

All chemicals and reagents were commercially available and used without further purification. Paramylon particles were obtained from *Euglena gracilis* in accordance with a previously reported method (Shibakami, Sohma, & Hayashi, 2012).

2.2. Visible absorption spectroscopy

A Congo red (CR) aqueous solution (0.032 mmol/l) was prepared by dissolving CR powder in water. Aqueous solutions with 0.25–1.0 mol/L NaOH and containing paramylon (10 mg/mL) were obtained by dissolving weighed amounts of paramylon particles in a 1.0-mol/L NaOH solution within less than 1 h and then diluting the solution with a given amount of water. Equal volumes of the CR solution and the paramylon solution, water, or a NaOH aqueous solution (0.25–1.0 mol/L) were well mixed, and the visible absorption spectra of these mixtures were immediately measured at room temperature with a Shimadzu UV-2500 spectrophotometer.

2.3. Circular dichroism spectroscopy

The samples used for circular dichroism (CD) spectroscopy were prepared in the same way as those for the visible absorption spectroscopic measurements. In brief, after equal volumes of the CR solution and the paramylon solution, or water were mixed, the CD spectra of the mixtures were immediately measured at room temperature using a JASCO J-820 spectropolarimeter.

2.4. Viscosity measurement

Aqueous solutions with 0.125–1.0 mol/L NaOH and containing paramylon (10 mg/mL) were prepared similarly to those for the visible absorption spectroscopic measurements. The viscosities of the solutions were determined using an A&D SV-1A vibratory viscometer, which measures viscosity by vibrating its sensor plates immersed in a sample at relatively low frequency (approximately 30 Hz) of sine-wave, at 25.3 ± 0.2 °C.

2.5. Nuclear magnetic resonance spectroscopy

The samples used for ^{13}C NMR spectroscopy were 0.20, 0.23, 0.25, 0.27, and 1.0 mol/L NaOH deuterium oxide solutions containing paramylon (10 mg/mL). The ^{13}C NMR spectra of the samples were measured with a Bruker AVANCE 500 spectrometer with 1,4-dioxane (10 mg/mL) as an internal reference.

2.6. Transmission electron microscopy

After a 0.97-mol/L NaOH aqueous solution containing paramylon (10 mg/mL) was prepared, it was immediately diluted with water in a stepwise manner to produce 0.49–0.049-mol/L solutions. Next, 2 μL of each solution was placed onto a hydrophilic copper grid processed by glow discharge for 2 min. Most of the excess solution on the grid was then removed with filter paper. Then, 2 μL of 0.3% 12-tungstophosphoric acid solution was applied to the grid as a staining agent. After 30 s, the excess solution was removed with filter paper. The prepared samples were observed using a JEOL 1010 transmission electron microscope at an accelerating voltage of 80 kV.

2.7. Light transmittance spectroscopy

Aqueous solutions with 0.25–1.0 mol/L NaOH and containing paramylon (10 mg/mL) were prepared similarly to those for the visible absorption spectroscopic measurements. The aqueous solution (0.65 mL) was then transferred in a cuvette (10 mm path length) and diluted with water (0.65 mL). Light transmittance spectrum was then measured using a Shimadzu UV-2500 spectrophotometer.

3. Results and discussion

3.1. Conformational analysis of paramylon

Although it has long been known that euglenoid algae produce paramylon particles (Gottlieb, 1850; Monfils, Triemer, & Bellairs, 2011) and that these particles are composed of a neutral linear β-1,3-glucan (Barras & Stone, 1968), there has been little or no research on paramylon conformation in solutions unlike other β-1,3-glucans. It has been anticipated that the formation of a paramylon nanofiber might be accompanied by a conformational change in the paramylon, so we performed conformational analysis before attempting to form a nanofiber. Specifically, we investigated whether or not paramylon adopts a helical conformation and if so, what external factors prompt the conformational change. We performed four types of measurement: visible absorption, CD, viscosity, and ^{13}C NMR.

3.1.1. Visible absorption spectrometry

In brief, the visible absorption spectra of a series of NaOH aqueous solutions containing CR in the presence and absence of paramylon were measured. It has been reported that if β-1,3-glucan helices form an inclusion complex with CR, the peak wavelength of the absorption maximum of the CR shifts (Ikeda & Shishido, 2005; Ogawa, Tsurugi et al., 1972; Saito et al., 1979; Saito, Ohki, Takasuka et al., 1977; Xu, Wang, Cai, & Zhang, 2010). As such, this visible absorption measurement has been a facile method for confirming the presence of helical conformation. Fig. 1 shows the relationship between the peak wavelength of the absorption maximum of the CR and NaOH concentration in the presence and absence of paramylon. In the presence of paramylon, the peak wavelength of the absorption maximum starts to shift just below a NaOH concentration of 0.25 mol/L, rapidly increases just below a NaOH concentration of 0.24 mol/L and almost reaches a plateau at 0.20 mol/L. A similar profile was observed in the visible absorption spectra of CR in the presence of curdlan (a linear β-1,3-glucan), which adopts helical and randomly coiled conformations respectively in dilute and thick alkaline solutions (Hara, Kiho, & Ukai, 1983; Ikeda & Shishido, 2005). When paramylon was not present in the solution, such rapid shifts were not observed: the peak wavelength of the absorption maxima gradually increased as the NaOH concentration decreased. In accordance with a previous study reporting that head-to-tail stacking of dyes (a J-type aggregate) leads to a red-shift in the absorption spectrum (James & Mees, 1966), the red-shift in this measurement indicates that paramylon starts to form a helix that accommodates CR molecules in a J-type

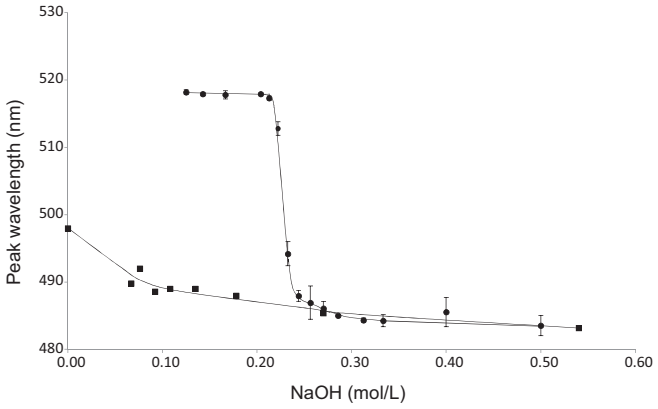

Fig. 1. Dependence of peak wavelength of absorption maximum of Congo red on NaOH concentration in presence (●) and absence (■) of paramylon. Data shown for presence of paramylon are average values with estimated standard deviations.

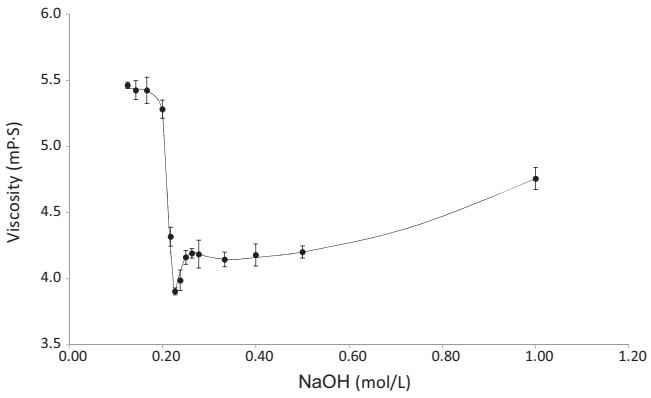

Fig. 3. Dependence of viscosity of alkaline solutions containing paramylon on NaOH concentration. Data are average values with estimated standard deviations.

fashion inside its cavity at 0.25 mol/L and that the transition to a helical conformation completed at 0.20 mol/L.

3.1.2. CD spectrometry

To confirm that paramylon adopts helical conformation, we measured the CD spectra of CR in the presence and absence of paramylon. CD spectroscopy is a useful method for examining the interaction between β-1,3-glucans and dye (Numata et al., 2006). No significant induced CD signal was observed in the absence of paramlon because of its optical inactiveness (data not shown). When CR was mixed with and 0.27-mol/L NaOH aqueous solution containing paramylon, CD signal did not appear (Fig. 2(a)). Slight dilution to 0.25 mol/L induced the appearance of a small split-type induced CD (Fig. 2(b)), and distinct signal was observed in a 0.24-mol/L NaOH solution (Fig. 2(c)). These results indicate that a well-ordered CR assembly is entrapped in the one-dimensional chiral cavity of the paramylon helix. Thus, these spectra indicate that paramylon starts to adopt a helical conformation at a NaOH concentration of 0.25 mol/L.

3.1.3. Viscometry

To gain insight into the paramylon conformation in solution, we measured the viscosities of a series of NaOH aqueous solutions containing paramylon. Viscosity measurement is a useful method for exploring the conformational transition of β-1,3-glucans in solution (Ogawa, Ono et al., 1972; Xu et al., 2010; Yanaki et al., 1981). Fig. 3 shows the dependence of the viscosity on the alkaline concentration. While the viscosity decreases from 4.76 to 4.20 mPa S as the NaOH concentration is reduced from 1.00 to 0.50 mol/L, the reason of which still remains to be unknown, it shows little change in the range of the NaOH concentration between 0.26 and 0.50 mol/L. Further dilution induced drastic changes in viscosity. In brief, the viscosity starts to decrease at 0.25 mol/L and it shows the minimal value at 0.23 mol/L. Slight additional dilution of the solution to 0.22 mol/L induces a sudden increase. Finally, the viscosity value reaches a plateau around 0.17–0.20 mol/L. This viscosity profile indicates that paramylon starts to change its assembling mode at 0.25 mol/L. Given that a paramylon polymer starts to change its conformation from a randomly coiled structure to a helix one at 0.25 mol/L, as suggested by visible absorption and CD spectroscopy, a plausible assembling mode that influences viscosity is a triple-helical structure. That is, it is plausible that paramylon starts to adopt a helical conformation at 0.25 mol/L and the transition completes around 0.17–0.20 mol/L. Previous studies reporting similar viscosity change profiles obtained with the triplex-forming β-1,3-glucans (Yanaki et al., 1981; Zhang, Li, Xu, & Zeng, 2005; Zhang et al., 2002), together with reports showing that a triplex structure has higher stability than a single-helix one (Ohno, Miura, Chiba, Adachi, & Yadomae, 1995; Young & Jacobs, 1998), support this hypothesis. The viscosity behavior in the range of the NaOH concentration between 0.20 and 0.25 mol/L is of interest. While it is plausible that the viscosity change stems from a combination of a decrease in the number of the randomly coiled polymer and a simultaneous increase in the number of the triplex, the detailed conformational change in this region still remains to be elucidated.

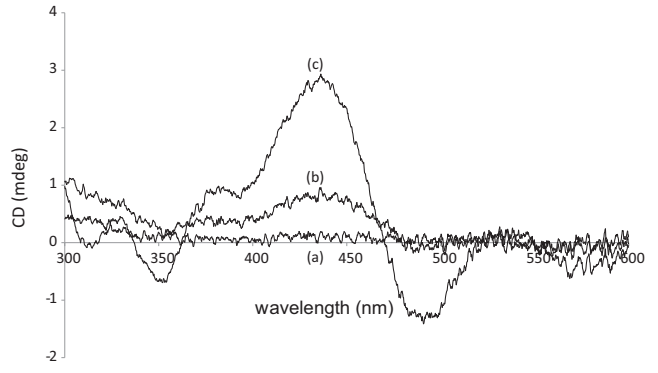

Fig. 2. CD signals of Congo red in alkaline solutions with NaOH concentrations of (a) 0.27, (b) 0.25, and (c) 0.24 mol/L in the presence of paramylon (10 mg/mL).

3.1.4. ^{13}C NMR spectrometry

To gain further insight into the paramylon conformation in alkaline solutions, we measured the ^{13}C NMR spectra of paramylon in solutions with different NaOH concentrations. ^{13}C NMR analysis is an effective method for evaluating polysaccharide conformation in solution (Saito, Ohki, & Sasaki, 1977; Saito et al., 1979; Saito, Ohki, Takasuka et al., 1977; Wang, Xu et al., 2009; Wang, Xu, & Zhang, 2008; Zhang et al., 2002). We used 0.20-, 0.23-, 0.25-, 0.27-, and 1.0-mol/L NaOH solutions for examining the transition from a randomly coiled structure to a helix one. Fig. 4(a) shows a ^{13}C NMR spectrum of paramylon in a 1.0-mol/L NaOH solution; in it, six distinct signals derived from the glucosyl residue are observed. The signals at 62.0, 69.5, 74.5, 77.3, 87.6, and 104.3 ppm are assigned to C6, C4, C2, C5, C3, and C1, respectively (Tamura, Wada, & Isogai, 2009). The narrow line width of the ^{13}C signals observed in this spectrum is characteristic of randomly coiled conformation (Saito, Ohki, & Sasaki, 1977). A similar spectrum was observed with a 0.27-mol/L solution (Fig. 4(b)). By contrast, as shown in Fig. 4(c and d), suppression of the ^{13}C NMR peaks of all glucosyl residues except for C6 starts around 0.25-mol/L, and further suppression was observed when the NaOH concentration was reduced to 0.23 mol/L. In

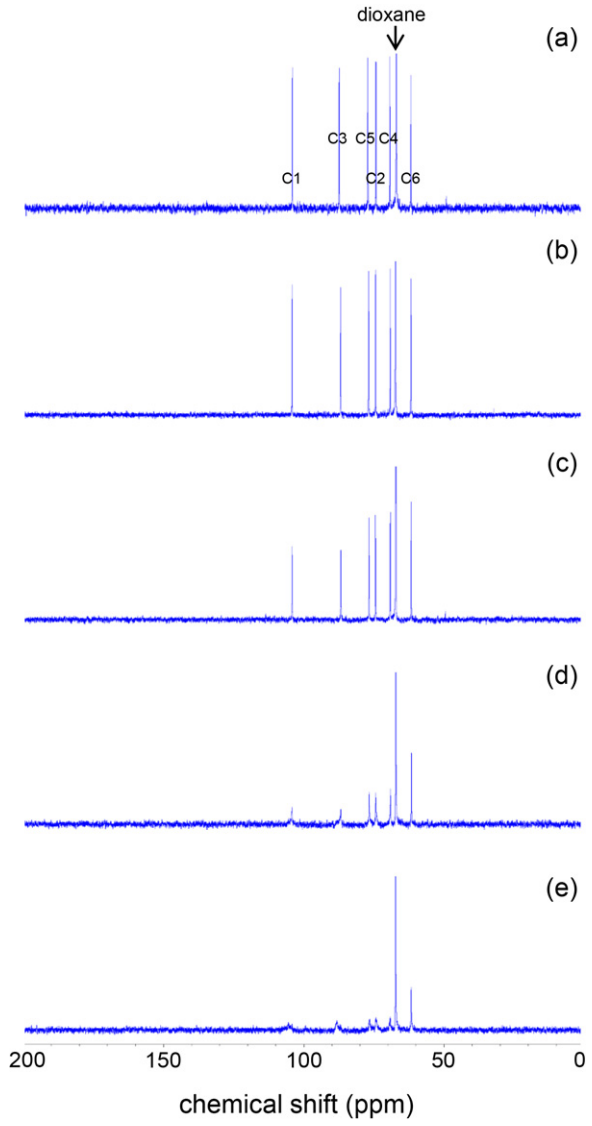

Fig. 4. ^{13}C NMR spectra of paramylon in alkaline solution for NaOH concentrations of (a) 1.0, (b) 0.27, (c) 0.25, (d) 0.23, and (e) 0.20 mol/L. Signal amplitude of all spectra is adjusted with reference to a 1,4-dioxane signal.

previous studies, the observable ^{13}C NMR signals were ascribed to single helices, and the signals of multiple helices were completely lost (Bryce, Mckinnon, Morris, Rees, & Thom, 1975; Chien & Wise, 1975; Saito, Ohki, & Sasaki, 1977; Smith, Jennings, & Deslauriers, 1975). Thus, this suppression indicates that the immobilization of the molecular chains by the formation of the triplex structure starts around 0.25 mol/L. Finally, considerable suppression was observed with a 0.20-mol/L solution, which implies that the immobilization completes around 0.20 mol/L. The relative insensitivity of the C6 peak intensity to NaOH concentration supports this speculation, assuming that C6 has higher flexibility than other carbons in the triple-helical form (Saito, Ohki, & Sasaki, 1977; Saito et al., 1979).

Given these findings from the visible absorption, viscosity, CD, and NMR measurements, we propose a transition process model in which randomly coiled β-1,3-glucan starts to transform into a triplex structure at 0.25 mol/L and completes the transition around 0.20 mol/L.

3.2. Preparation of paramylon nanofibers

Many of the procedures reported for preparing micro- and nanofibers primarily hinge on the association of randomly coiled β-1,3-glucans that are dissolved in an alkaline solution by reducing the NaOH concentration (Dobashi, Nobe, Yoshihara, Yamamoto, & Konno, 2004; Gagnon & Lafleur, 2009; Koreeda, Harada, Ogawa, Sato, & Kasai, 1974; Marchessault & Deslandes, 1979; Xu et al., 2010; Zhang, Xu, & Zhang, 2008). In this study, we examined the feasibility of the dilution method. Our primary objectives were to determine if paramylon forms a nanofiber using a transmission electron microscope, and if so, to estimate the onset NaOH concentration for the paramylon nanofiber formation. In brief, stepwise dilution with water of a 0.97-mol/L NaOH solution containing paramylon (10 mg/mL) provided a series of alkaline solutions with different NaOH concentrations (0.049 to 0.49 mol/L) and different paramylon concentrations (5.0–0.5 mg/mL). As shown in Fig. 5, the 0.049-, 0.10-, and 0.19-mol/L NaOH solutions contained similar well-defined nanofibers with a width of ca. 20 nm, while no such nanofibers were observed in the 0.29- and 0.49-mol/L NaOH solutions under a microscope (data not shown). These results suggest that the onset NaOH concentration for the formation of a well-defined paramylon nanofiber is below 0.19 mol/L. To see if paramylon solutions with higher NaOH concentrations contain the nanofibers, additional microscopic observations were carried out. We did not observe any nanofibers in the 0.21-, 0.22-, and 0.23-mol/L NaOH solutions. These results indicate that the onset NaOH concentration for the paramylon nanofiber formation is approximately 0.19–0.21 mol/L.

3.3. Structure of paramylon nanofibers

Next we explored the structure of the paramylon nanofibers in detail. Micrographs of well-defined nanofibers revealed that the nanofibers had a high aspect ratio with a length of more than several micrometers and a width of 18.8 ± 3.3 nm. The nanofiber width

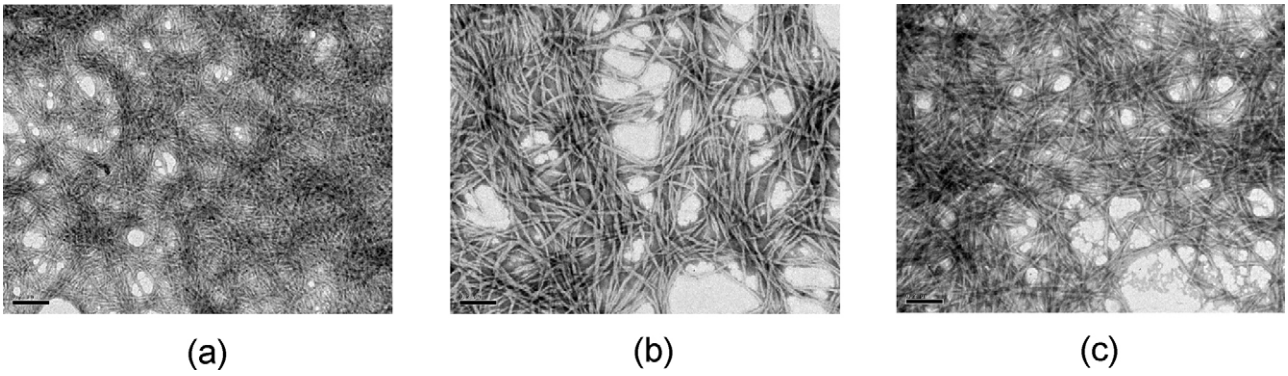

Fig. 5. TEM images of paramylon nanofibers in alkaline solutions with NaOH concentrations of (a) 0.049, (b) 0.10, and (c) 0.19. Scale bar represents 200 nm.

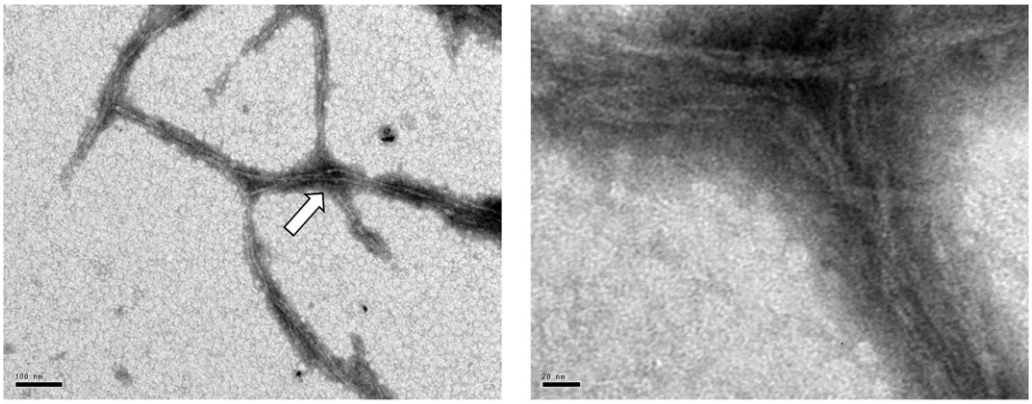

Fig. 6. TEM images of unfolded paramylon nanofibers in 0.10-mol/L NaOH solution: (a) low magnification image and (b) high magnification image of nanofibers indicated by white arrow in (a). Scale bar represents 100 mm for (a) and 20 nm for (b).

was substantially constant regardless of the NaOH concentration and the paramylon concentration and is comparable to that of previously reported curdlan nanofibers (Harada, Kanzawa, Kanenaga, Koreeda, & Harada, 1991; Kanzawa, Harada, Koreeda, Harada, & Okuyama, 1989; Koreeda et al., 1974; Marchessault & Deslandes, 1979; Takahashi, Harada, Koreeda, & Harada, 1986). A previous X-ray diffraction study on the crystal structure of paramylon revealed that the hexagonal unit cell of its triplex structure had dimensions of $a = b = 1.556 \pm 0.005$ nm and $c = 1.878 \pm 0.005$ nm (Chuah et al., 1983). On the basis of a comparison of these unit cell lengths with the width of the nanofiber, we think that more than about one hundred triplex structures are bundled in a nanofiber approximately 20 nm thick. While a magnified image of nanofibers in the 0.10-mol/L solution does not show the triplex structure, it does show unfolded nanofibers with a width of ca. 4 nm (Fig. 6). This microscopic image confirms that a paramylon nanofiber is indeed formed by the bundling of the thin nanofibers. Previous X-ray and TEM studies revealed a higher order formation of paramylon in a native paramylon particle, in which thin fibers with a diameter of 4 nm are bundled into a thicker fiber (Kiss, Vasconcelos, & Triemer, 1987; Marchessault & Deslandes, 1979). It is likely that a similar higher order formation occurs in vitro. To examine the polysaccharide aggregation mode, we measured the light transmittance spectra of alkaline solutions containing paramylon. The spectra are shown in Fig. 7. Apparently, the solutions with the NaOH concentration of 0.50 and 0.25 mol/L had similar light transmittance, indicating that many paramylon molecules still adopt a randomly coiled conformation at 0.25 mol/L. Comparison of the spectra measured at 0.20 and 0.125 mol/L shows that the light transmittance of 0.125-mol/L solution is lower than that of 0.20-mol/L one, which implies that the polysaccharide aggregation progressed as the NaOH concentration was reduced from 0.20 to 0.125 mol/L.

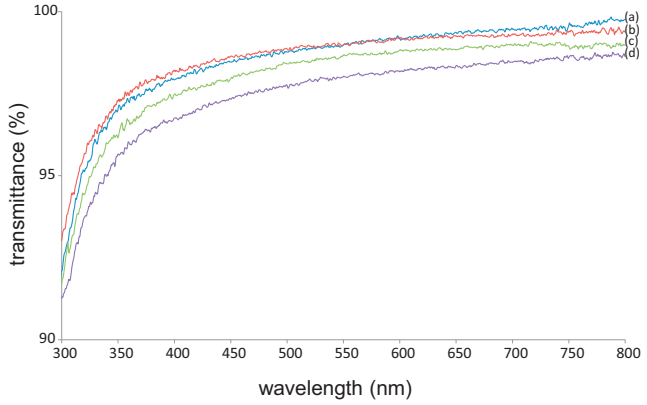

Fig. 7. Light transmittance spectra of alkaline solutions with NaOH concentrations of (a) 0.50, (b) 0.25, (c) 0.20, and (d) 0.125 mol/L and containing paramylon (5 mg/mL).

3.4. Formation of paramylon nanofibers

Comparison of the micrographs with the absorption, CD, viscosity, NMR, and light transmittance measurement results provides a clue to understanding the stepwise formation of nanofibers. As mentioned in section 3.1.4, randomly coiled paramylon starts to associate into a triplex at a NaOH concentration of 0.25 mol/L and the association completes around 0.20 mol/L. This is apparently the first assembly step. The consideration of a plausible second assembly step is as follows. It is noteworthy that the micrographs of the 0.21-, 0.22- and 0.23-mol/L NaOH solutions did not show any nanofiber structures, while the peak wavelength of the absorption maximum, CD signal, and viscosity are in the process of change in this concentration region. Thus, this comparison, together with the fact that the 0.19-mol/L solution contains the 20-nm-width nanofibers, suggests that the triplex associates to form the 20-nm-width nanofiber around 0.19 mol/L. It is also noteworthy that no separate 4-nm-width nanofibers were observed in the range between 0.21 and 0.23 mol/L under a microscope. Thus, we think that the transition from the triplex to the 20-nm-width nanofiber occurs around 0.19 mol/L. As the light transmittance spectroscopic results show, it is plausible that the nanofibers gradually aggregate as the NaOH concentration was reduced from 0.20 to 0.125 mol/L. While this thickening may be a plausible third assembly process, the detailed mechanism still remains to be elucidated.

3.5. Association mode of paramylon nanofibers

Examination of these microscopic images also provides a clue to understanding the association modes of paramylon polymers. As mentioned in Section 3.3, the thinnest nanofiber that was observed under a microscope had a width of ca. 4 nm while most nanofibers had an eventual width of ca. 20 nm. These results indicate that a fiber with a width of ca. 4 nm is the minimal assembly unit of the paramylon triplex structure and that the final result is a nanofiber with a width of ca. 20 nm. The discontinuous change in width suggests that the nanofibers have an ordered structure at each stage of assembly. Although their detailed structure remains to be elucidated, a plausible hierarchic association mode is that seven triplex structures assemble into a cylindrical nanofiber about 4 nm

wide and that seven of these nanofibers, in turn, assemble into a nanofiber about 20 nm wide.

4. Conclusion

Although paramylon has long been known to be a β-1,3-glucan, this is the first report on the formation of a polysaccharide nanofiber formed by a self-assembly process in vitro as far as we are aware. Of particular note in the nanofiber morphology is the narrow distribution in width. This structural feature is attributed primarily to the use of a bottom-up approach in which components automatically self-assemble into well-organized structures. This approach can thus be differentiated from the top-down approach, which has frequently been used for cellulose nanofiber preparation. Efforts currently in progress are aimed at identifying potential biological applications of paramylon nanofibers. The results of these studies will be reported in due course.

Acknowledgments

This research was partly supported by the Advanced Low Carbon Technology Research and Development Program of the Japan Science and Technology Agency.

References

Abe, K., Iwamoto, S., & Yano, H. (2007). Obtaining cellulose nanofibers with a uniform width of 15 nm from wood. *Biomacromolecules*, *8*(10), 3276–3278. http://dx.doi.org/10.1021/Bm700624p

Barras, D. R., & Stone, B. A. (1968). *Carbohydrate composition and metabolism* New York: Academic Press.

Barsanti, L., Vismara, R., Passarelli, V., & Gualtieri, P. (2001). Paramylon (beta-1,3-glucan) content in wild type and WZSL mutant of *Euglena gracilis*. Effects of growth conditions. *Journal of Applied Phycology*, *13*(1), 59–65.

Bhatnagar, A., & Sain, M. (2005). Processing of cellulose nanofiber-reinforced composites. *Journal of Reinforced Plastics and Composites*, *24*(12), 1259–1268. http://dx.doi.org/10.1177/0731684405049864

Booy, F. P., Chanzy, H., & Boudet, A. (1981). An electron-diffraction study of paramylon storage granules from *Euglena gracilis*. *Journal of Microscopy-Oxford*, *121*(Feb), 133–140.

Brandes, D., Buetow, D. E., Bertini, F., & Malkoff, D. B. (1964). Role of lysosomes in cellular lytic processes. I. Effect of carbon starvation in *Euglena gracilis*. *Experimental and Molecular Pathology*, *3*(6), 583–609.

Bryce, T. A., Mckinnon, A. A., Morris, E. R., Rees, D. A., & Thom, D. (1975). Chain conformations in sol–gel transitions for polysaccharide systems, and their characterization by spectroscopic methods. *Faraday Discussions*, *57*, 221–229.

Chakraborty, A., Sain, M., & Kortschot, M. (2005). Cellulose microfibrils: A novel method of preparation using high shear refining and cryocrushing. *Holzforschung*, *59*(1), 102–107. http://dx.doi.org/10.1515/Hf.2005.016

Chen, Z. G., Wang, P. W., Wei, B., Mo, X. M., & Cui, F. Z. (2010). Electrospun collagen-chitosan nanofiber: A biomimetic extracellular matrix for endothelial cell and smooth muscle cell. *Acta Biomaterialia*, *6*(2), 372–382. http://dx.doi.org/10.1016/j.actbio.2009.07.024

Chien, J. C. W., & Wise, W. B. (1975). C-13 nuclear magnetic-resonance and circular-dichroism study of collagen-gelatin transformation in enzyme solubilized collagen. *Biochemistry*, *14*(12), 2786–2792.

Chuah, C. T., Sarko, A., Deslandes, Y., & Marchessault, R. H. (1983). Packing analysis of carbohydrates and polysaccharides. Part 14. Triple-helical crystalline-structure of curdlan and paramylon hydrates. *Macromolecules*, *16*(8), 1375–1382.

Clarke, A. E., & Stone, B. A. (1960). Structure of the paramylon from *Euglena gracilis*. *Biochimica Et Biophysica Acta*, *44*(1), 161–163.

Cooper, A., Zhong, C., Kinoshita, Y., Morrison, R. S., Rolandi, M., & Zhang, M. Q. (2012). Self-assembled chitin nanofiber templates for artificial neural networks. *Journal of Materials Chemistry*, *22*(7), 3105–3109. http://dx.doi.org/10.1039/C2jm15487k

Dobashi, T., Nobe, M., Yoshihara, H., Yamamoto, T., & Konno, A. (2004). Liquid crystalline gel with refractive index gradient of curdlan. *Langmuir*, *20*(16), 6530–6534. http://dx.doi.org/10.1021/La035822z

Falch, B. H., & Stokke, B. T. (2001). Structural stability of (1→3)-beta-D-glucan macrocycles. *Carbohydrate Polymers*, *44*(2), 113–121. http://dx.doi.org/10.1016/S0144-8617(00)00214-9

Gagnon, M. A., & Lafleur, M. (2009). Self-diffusion and mutual diffusion of small molecules in high-set curdlan hydrogels studied by P-31 NMR. *Journal of Physical Chemistry B*, *113*(27), 9084–9091. http://dx.doi.org/10.1021/Jp81105p

Gottlieb, J. (1850). Ueber eine neue, mit Starkmehl isomere Substanz. *Annalen der chemie und pharmacie*, *75*, 51–61.

Hara, C., Kiho, T., & Ukai, S. (1983). Polysaccharides in fungi.15. A branched (1→3)-beta-D-glucan from a sodium-carbonate extract of dictyophora-indusiata fisch. *Carbohydrate Research*, *117*(Jun), 201–213.

Harada, T., Kanzawa, Y., Kanenaga, K., Koreeda, A., & Harada, A. (1991). Electron-microscopic studies on the ultrastructure of curdlan and other polysaccharides in gels used in foods. *Food Structure*, *10*(1), 1–18.

Harada, T., Misaki, A., & Saito, H. (1968). Curdlan: A bacterial gel-forming beta-1 3-glucan. *Archives of Biochemistry and Biophysics*, *124*(1–3), 292–298.

Hong, J. P., Um, M. C., Nam, S. R., Hong, J. I., & Lee, S. (2009). Organic single-nanofiber transistors from organogels. *Chemical Communications*, (3), 310–312. http://dx.doi.org/10.1039/B816030a

Ikeda, S., & Shishido, Y. (2005). Atomic force microscopy studies on heat-induced gelation of curdlan. *Journal of Agricultural and Food Chemistry*, *53*(3), 786–791. http://dx.doi.org/10.1021/Jf048797r

Iwatake, A., Nogi, M., & Yano, H. (2008). Cellulose nanofiber-reinforced polylactic acid. *Composites Science and Technology*, *68*(9), 2103–2106. http://dx.doi.org/10.1016/j.compscitech.2008.03.006

James, T. H., & Mees, C. E. K. (1966). *The theory of the photographic process* (3d ed.). New York: Macmillan.

Kanzawa, Y., Harada, T., Koreeda, A., Harada, A., & Okuyama, K. (1989). Difference of molecular association in 2 types of curdlan gel. *Carbohydrate Polymers*, *10*(4), 299–313.

Kashiwagi, Y., Norisuye, T., & Fujita, H. (1981). Triple helix of schizophyllum-commune polysaccharide in dilute-solution. 4. Light-scattering and viscosity in dilute aqueous sodium-hydroxide. *Macromolecules*, *14*(5), 1220–1225.

Kim, I. D., Rothschild, A., Lee, B. H., Kim, D. Y., Jo, S. M., & Tuller, H. L. (2006). Ultrasensitive chemiresistors based on electrospun TiO2 nanofibers. *Nano Letters*, *6*(9), 2009–2013. http://dx.doi.org/10.1021/Nl061197h

Kiss, J. Z., Vasconcelos, A. C., & Triemer, R. E. (1987). Structure of the euglenoid storage carbohydrate, paramylon. *American Journal of Botany*, *74*(6), 877–882.

Kobayashi, K., Kimura, S., Togawa, E., Wada, M., & Kuga, S. (2010). Crystal transition of paramylon with dehydration and hydration. *Carbohydrate Polymers*, *80*(2), 491–497. http://dx.doi.org/10.1016/j.carbpol.2009.12.009

Koreeda, A., Harada, T., Ogawa, K., Sato, S., & Kasai, N. (1974). Study of ultrastructure of gel-forming (1→3)-beta-D-glucan(curdlan-type polysaccharide) by electron-microscopy. *Carbohydrate Research*, *33*(2), 396–399.

Kreger, D. R., & Meeuse, B. J. D. (1952). X-ray diagrams of Euglena-paramylon, of the acid-insoluble glucan of yeast cell walls and of laminarin. *Biochimica Et Biophysica Acta*, *9*(6), 699–700.

Li, D., & Kaner, R. B. (2005). Processable stabilizer-free polyaniline nanofiber aqueous colloids. *Chemical Communications*, (26), 3286–3288. http://dx.doi.org/10.1039/B504020e

Loscertales, I. G., Barrero, A., Marquez, M., Spretz, R., Velarde-Ortiz, R., & Larsen, G. (2004). Electrically forced coaxial nanojets for one-step hollow nanofiber design. *Journal of the American Chemical Society*, *126*(17), 5376–5377. http://dx.doi.org/10.1021/Ja049443j

Marchessault, R. H., & Deslandes, Y. (1979). Fine-structure of (1→3)-beta-D-glucans: Curdlan and paramylon. *Carbohydrate Research*, *75*(Oct), 231L 242.

McIntosh, M., Stone, B. A., & Stanisich, V. A. (2005). Curdlan and other bacterial (1→3)-beta-D-glucans. *Applied Microbiology and Biotechnology*, *68*(2), 163–173. http://dx.doi.org/10.1007/s00253-005-1959-5

Monfils, A. K., Triemer, R. E., & Bellairs, E. F. (2011). Characterization of paramylon morphological diversity in photosynthetic euglenoids (Euglenales, Euglenophyta). *Phycologia*, *50*(2), 156–169. http://dx.doi.org/10.2216/09-112.1

Numata, M., Tamesue, S., Fujisawa, T., Haraguchi, S., Hasegawa, T., Bae, A. H., & Shinkai, S. (2006). Beta-1,3-glucan polysaccharide (schizophyllan) acting as a one-dimensional host for creating supramolecular dye assemblies. *Organic Letters*, *8*(24), 5533–5536. http://dx.doi.org/10.1021/Ol062229a

Ogawa, K., Ono, S., Watanabe, T., & Tsurugi, J. (1972). Conformational behavior of a gel-forming (1→3)-beta-D-glucan in alkaline solution. *Carbohydrate Research*, *23*(3), 399–405.

Ogawa, K., Tsurugi, J., & Watanabe, T. (1972). Complex of gel-forming beta-1,3-D-glucan with congo-red in alkaline solution. *Chemistry Letters*, (8), 689–692.

Ohkawa, K., Minato, K. I., Kumagai, G., Hayashi, S., & Yamamoto, H. (2006). Chitosan nanofiber. *Biomacromolecules*, *7*(11), 3291–3294. http://dx.doi.org/10.1021/Bm0604395

Ohno, N., Miura, N. N., Chiba, N., Adachi, Y., & Yadomae, T. (1995). Comparison of the immunopharmacological activities of triple and single-helical schizophyllan in mice. *Biological & Pharmaceutical Bulletin*, *18*(9), 1242–1247.

Paakko, M., Ankerfors, M., Kosonen, H., Nykanen, A., Ahola, S., Osterberg, M., & Lindstrom, T. (2007). Enzymatic hydrolysis combined with mechanical shearing and high-pressure homogenization for nanoscale cellulose fibrils and strong gels. *Biomacromolecules*, *8*(6), 1934–1941. http://dx.doi.org/10.1021/bm061215p

Saito, H., Misaki, A., & Harada, T. (1968). A compararison of structure of curdlan pachyman. *Agricultural and Biological Chemistry*, *32*(10), 1261–1269.

Saito, H., Ohki, T., & Sasaki, T. (1977). C-13 nuclear magnetic-resonance study of gel-forming (1→3)-beta-D-glucans: Evidence of presence of single-helical conformation in a resilient gel of a curdlan-type polysaccharide-13140 from alcaligenes-faecalis-var-myxogenes-Ifo13140. *Biochemistry*, *16*(5), 908–914.

Saito, H., Ohki, T., & Sasaki, T. (1979). C-13-nuclear magnetic-resonance study of polysaccharide gels: Molecular architecture in the gels consisting of fungal, branched (1→3)-beta-D-glucans (lentinan and schizophyllan) as manifested by conformational-changes induced by sodium-hydroxide. *Carbohydrate Research*, *74*(Sep), 227–240.

Saito, H., Ohki, T., Takasuka, N., & Sasaki, T. (1977). C-13-Nmr-spectral study of a gel-forming, branched (1→3)-beta-D-glucan, (lentinan) from lentinus-edodes,

and its acid-degraded fractions: Structure, and dependence of conformation on molecular-weight. *Carbohydrate Research*, *58*(2), 293–305.

Saito, T., & Isogai, A. (2004). TEMPO-mediated oxidation of native cellulose. The effect of oxidation conditions on chemical and crystal structures of the water-insoluble fractions. *Biomacromolecules*, *5*(5), 1983–1989.

Santek, B., Friehs, K., Lotz, M., & Flaschel, E. (2012). Production of paramylon, a ss-1,3-glucan, by heterotrophic growth of *Euglena gracilis* on potato liquor in fed-batch and repeated-batch mode of cultivation. *Engineering in Life Sciences*, *12*(1), 89–94. http://dx.doi.org/10.1002/elsc.201100025

Shibakami, M., Sohma, M., & Hayashi, M. (2012). Fabrication of doughnut-shaped particles from spheroidal paramylon granules of *Euglena gracilis* using acetylation reaction. *Carbohydrate Polymers*, *87*(1), 452–456. http://dx.doi.org/10.1016/j.carbpol.2011.08.012

Smith, I. C. P., Jennings, H. J., & Deslauriers, R. (1975). C-13 nuclear magnetic-resonance and conformations of biological molecules. *Accounts of Chemical Research*, *8*(9), 306–313.

Stokke, B. T., Falch, B. H., & Dentini, M. (2001). Macromolecular triplex zipping observed in derivatives of fungal (1 → 3)-beta-D-glucan by electron and atomic force microscopy. *Biopolymers*, *58*(6), 535–547. Doi 10.1002/1097-0282(200105)58:6<535::Aid-Bip1029>3.0.Co;2-S.

Takahashi, F., Harada, T., Koreeda, A., & Harada, A. (1986). Structure of curdlan that is resistant to (1 → 3)beta-D-glucanase. *Carbohydrate Polymers*, *6*(6), 407–421.

Tamura, N., Wada, M., & Isogai, A. (2009). TEMPO-mediated oxidation of (1 → 3)-beta-D-glucans. *Carbohydrate Polymers*, *77*(2), 300–305. http://dx.doi.org/10.1016/j.carbpol.2008.12.040

Taniguchi, T., & Okamura, K. (1998). New films produced from microfibrillated natural fibres. *Polymer International*, *47*(3), 291–294, doi: 10.1002/(sici)1097-0126(199811)47:3 < 291::aid-pi11 > 3.0.co;2-1.

Wang, J. T., Xu, X. J., Zheng, H., Li, J. L., Deng, C., Xu, Z. H., & Chen, J. H. (2009). Structural characterization, chain conformation, and morphology of a beta-(1 → 3)-D-glucan isolated from the fruiting body of Dictyophora indusiata. *Journal of Agricultural and Food Chemistry*, *57*(13), 5918–5924. http://dx.doi.org/10.1021/Jf9009872

Wang, X. H., Xu, X. J., & Zhang, L. (2008). Thermally induced conformation transition of triple-helical lentinan in NaCl aqueous solution. *Journal of Physical Chemistry B*, *112*(33), 10343–10351. http://dx.doi.org/10.1021/Jp802174v

Wang, X. H., Zhang, Y. Y., Zhang, L. N., & Ding, Y. W. (2009). Multiple conformation transitions of triple helical lentinan in DMSO/water by microcalorimetry. *Journal of Physical Chemistry B*, *113*(29), 9915–9923. http://dx.doi.org/10.1021/Jp811289y

Wnek, G. E., Carr, M. E., Simpson, D. G., & Bowlin, G. L. (2003). Electrospinning of nanofiber fibrinogen structures. *Nano Letters*, *3*(2), 213–216. http://dx.doi.org/10.1021/Nl025866c

Xu, X. J., Wang, X. H., Cai, F., & Zhang, L. N. (2010). Renaturation of triple helical polysaccharide lentinan in water-diluted dimethylsulfoxide solution. *Carbohydrate Research*, *345*(3), 419–424. http://dx.doi.org/10.1016/j.carres.2009.10.013

Yanaki, T., Kojima, T., & Norisuye, T. (1981). Triple helix of scleroglucan in dilute aqueous sodium-hydroxide. *Polymer Journal*, *13*(12), 1135–1143.

Young, S. H., & Jacobs, R. R. (1998). Sodium hydroxide-induced conformational change in schizophyllan detected by the fluorescence dye, aniline blue. *Carbohydrate Research*, *310*(1-2), 91–99.

Zhang, L., Li, X. L., Xu, X. J., & Zeng, F. B. (2005). Correlation between antitumor activity, molecular weight, and conformation of lentinan. *Carbohydrate Research*, *340*(8), 1515–1521. http://dx.doi.org/10.1016/j.carres.2005.02.032

Zhang, L., Li, X. L., Zhou, Q., Zhang, X. F., & Chen, R. Q. (2002). Transition from triple helix to coil of Lentinan in solution measured by SEC, viscometry, and C-13 NMR. *Polymer Journal*, *34*(6), 443–449.

Zhang, L. N., Zhang, X. F., Zhou, Q., Zhang, P. Y., Zhang, M., & Li, X. L. (2001). Triple helix of beta-D-glucan from Lentinus Edodes in 0.5 M NaCl aqueous solution characterized by light scattering. *Polymer Journal*, *33*(4), 317–321.

Zhang, T. J., Wang, W., Zhang, D. Y., Zhang, X. X., Ma, Y. R., Zhou, Y. L., & Qi, L. M. (2010). Biotemplated synthesis of gold nanoparticle-bacteria cellulose nanofiber nanocomposites and their application in biosensing. *Advanced Functional Materials*, *20*(7), 1152–1160. http://dx.doi.org/10.1002/adfm.200902104

Zhang, X. Y., Goux, W. J., & Manohar, S. K. (2004). Synthesis of polyaniline nanofibers by "nanofiber seeding". *Journal of the American Chemical Society*, *126*(14), 4502–4503. http://dx.doi.org/10.1021/Ja031867a

Zhang, Y. Y., Li, S., & Zhang, L. N. (2010). Aggregation behavior of triple helical polysaccharide with low molecular weight in diluted aqueous solution. *Journal of Physical Chemistry B*, *114*(15), 4945–4954. http://dx.doi.org/10.1021/Jp9100398

Zhang, Y. Y., Xu, X. J., & Zhang, L. (2008). Gel formation and low-temperature intramolecular conformation transition of a triple-helical polysaccharide lentinan in water. *Biopolymers*, *89*(10), 852–861. http://dx.doi.org/10.1002/Bip.21025

Zhao, H.-P., Feng, X.-Q., & Gao, H. (2007). Ultrasonic technique for extracting nanofibers from nature materials. *Applied Physics Letters*, *90*(7) http://dx.doi.org/10.1063/1.2450666